

# Hof1 plays a checkpoint-related role in MMS-induced DNA damage response in *Candida albicans*

Jinrong Feng<sup>a</sup>, Amjad Islam<sup>b,c</sup>, Bjorn Bean<sup>b</sup>, Jia Feng<sup>a</sup>, Samantha Sparapani<sup>b</sup>, Manjari Shrivastava<sup>b</sup>, Aashima Goyal<sup>d</sup>, Raha Parvizi Omran<sup>b</sup>, Jaideep Mallick<sup>e</sup>, and Malcolm Whiteway<sup>b,\*</sup>

<sup>a</sup>Department of Pathogen Biology, School of Medicine, Nantong University, Nantong, Jiangsu 226001, China;

<sup>b</sup>Biology Department, Concordia University, Montreal, QC H4B 1R6, Canada; <sup>c</sup>Department of Biochemistry and Biophysics, University of Rochester Medical Center, Rochester, NY 14642; <sup>d</sup>Department of Biochemical Engineering and Biotechnology, Indian Institute of Technology Delhi, New Delhi 110 016, India; <sup>e</sup>Department of Microbiology and Immunology, Faculty of Medicine, Université Laval, Québec, QC G1V 4G2, Canada

**ABSTRACT** Cells depend on robust DNA damage recognition and repair systems to maintain genomic integrity for survival in a mutagenic environment. In the pathogenic yeast *Candida albicans*, a subset of genes involved in the response to DNA damage-induced genome instability and morphological changes has been found to regulate virulence. To better understand the virulence-linked DNA repair network, we screened for methyl methane sulfonate (MMS) sensitivity within the GRACE conditional expression collection and identified 56 hits. One of these potential DNA damage repair-associated genes, a *HOF1* conditional mutant, unexpectedly had a previously characterized function in cytokinesis. Deletion of *HOF1* resulted in MMS sensitivity and genome instability, suggesting Hof1 acts in the DNA damage response. By probing genetic interactions with distinct DNA repair pathways, we found that Hof1 is genetically linked to the Rad53 pathway. Furthermore, Hof1 is down-regulated in a Rad53-dependent manner and its importance in the MMS response is reduced when Rad53 is overexpressed or when *RAD4* or *RAD23* is deleted. Together, this work expands our understanding of the *C. albicans* DNA repair network and uncovers interplay between the cytokinesis regulator Hof1 and the Rad53-mediated checkpoint.

**Monitoring Editor**  
Yixian Zheng  
Carnegie Institution

Received: Jun 14, 2019  
Revised: Nov 26, 2019  
Accepted: Jan 6, 2020

## INTRODUCTION

To remain viable, cells must maintain genomic integrity, but both external and internal factors such as radiation, replication errors, and reactive oxygen species can cause DNA damage that compromises this integrity (Hoeijmakers, 2009). By creating chromosomal abnormalities, DNA damage can disrupt cell function, potentially resulting in cancer or cell death (Hoeijmakers, 2009). To defend against such events, cells have evolved molecular mechanisms to recognize and

repair damaged DNA, improving the fidelity of genetic information transfer between generations (Zhou and Elledge, 2000; Wood *et al.*, 2001).

Past studies have applied a well-developed genetic and molecular toolkit to characterize the DNA damage response in the ascomycete yeast *Saccharomyces* (Schwartz *et al.*, 2002; Boiteux and Jinks-Robertson, 2013). Experimentally, DNA damage is often induced with methyl methane sulfonate (MMS), a methylating agent that modifies both guanine and adenine, causing base mispairing and ultimately double-strand breaks (Lundin *et al.*, 2005; Shi *et al.*, 2007). Once DNA is damaged, a cell employs diverse set of proteins to recognize the damage, pause the cell cycle and DNA replication, activate the proper repair machinery, and restart the cell cycle after the repair (Sirbu and Cortez, 2013).

Activation of signaling pathways termed checkpoints pauses cellular processes, allowing time for DNA repair (Zhou and Elledge, 2000). In particular, the activation pathway of the checkpoint kinase Rad53 has been well studied (Pelliccioli and Foiani, 2005; Sweeney *et al.*, 2005; Branzei and Foiani, 2006; Conde *et al.*, 2010;

This article was published online ahead of print in MBoC in Press (<http://www.molbiolcell.org/cgi/doi/10.1091/mbc.E19-06-0316>) on January 15, 2020.

\*Address correspondence to: Malcolm Whiteway ([malcolm.whiteway@concordia.ca](mailto:malcolm.whiteway@concordia.ca)).

Abbreviations used: BER, base excision repair; DAPI, 4', 6'-diamidino-2-phenylindole dihydrochloride; DIC, differential interference contrast; HU, hydroxyurea; IP, immunoprecipitation; MMS, methyl methane sulfonate; NER, nucleotide excision repair; WT, wild type; YNB, yeast nitrogen base.

© 2020 Feng *et al.* This article is distributed by The American Society for Cell Biology under license from the author(s). Two months after publication it is available to the public under an Attribution–Noncommercial–Share Alike 3.0 Unported Creative Commons License (<http://creativecommons.org/licenses/by-nc-sa/3.0>).

"ASCB®," "The American Society for Cell Biology®," and "Molecular Biology of the Cell®" are registered trademarks of The American Society for Cell Biology.

Chen *et al.*, 2015). First, sensors such as Tel1 and Mec1 receive the signal from damaged DNA (Sanchez *et al.*, 1996; Baroni *et al.*, 2004) and, with the help of adaptor proteins Mrc1 or Rad9 (Murakami-Sekimata *et al.*, 2010; Berens and Toczyski, 2012; Ohouo *et al.*, 2013; Bacal *et al.*, 2018), phosphorylate Rad53. Phosphorylated Rad53 then auto-phosphorylates to generate the active form of the kinase (Heideker *et al.*, 2007). Activated Rad53 interrupts the cell cycle and regulates the downstream target proteins required to repair the damage. Rad53 has also been implicated in modulating morphology, potentially through interactions with septins (Smolka *et al.*, 2006). Deletion of Rad53, or other checkpoint kinases like Rad9 and Mrc1, prevents coordination of the repair process and therefore results in a strong sensitivity to DNA-damaging reagents like MMS (Weinert *et al.*, 1994; Hanway *et al.*, 2002; Kitanovic and Wolff, 2006).

After checkpoint activation, distinct pathways are involved in repairing the DNA damage. The base excision repair (BER) pathway, the Rad52-related recombination epistasis group (Kwon and Sung, 2017), and the Rad6 epistasis group take part in the response to MMS-induced DNA damage (Somasagara *et al.*, 2017). The BER pathway, initiated by a DNA glycosylase that recognizes and removes the damaged or abnormal base, leaving an abasic site, is mainly used to repair damage that creates minor disturbances in the DNA helix (Memisoglu and Samson, 2000). The abasic site is further processed by either short-patch BER (for replacement of 1 nucleotide) or long-patch BER (for replacement of 2–13 nucleotides). The RAD6 group represents a postreplication repair pathway and includes genes encoding specialized translesion synthesis polymerases, able to replicate through DNA damage (Lawrence, 1994). Furthermore, mutants lacking some components of other repair pathways, like the Rad14-related nucleotide excision repair (NER) process (Prakash and Prakash, 2000), are also MMS sensitive, highlighting the diversity of proteins required to recognize and correct MMS-induced damage. After DNA repair, the checkpoint kinase must be deactivated to allow the cell to resume the cell cycle. This process is mediated by protein phosphatases including Pph3 and Ptc2/Ptc3 (Leroy *et al.*, 2003; O’Neill *et al.*, 2007; Kim *et al.*, 2011), which are important for the recovery from, or adaptation to, MMS-induced DNA damage.

*Candida albicans* is one of the most common fungal pathogens, and its pathogenicity is related to characteristics such as adhesion to and invasion of host cells, the secretion of hydrolases, the yeast-to-hypha transition, contact sensing/thigmotropism, and biofilm formation (Whiteway and Bachewich, 2007). DNA damage in *C. albicans* causes genome instability and abnormal growth (Loll-Kripplleber *et al.*, 2014). *C. albicans* yeast cells treated with either the DNA-replication inhibitor hydroxyurea (HU) or the DNA methylation agent MMS exhibit activation of the checkpoint kinase Rad53 accompanied by significant filamentous growth (Shi *et al.*, 2007). Similarly, deletion of RAD52 causes a strong sensitivity to MMS and activates filamentous growth (Andaluz *et al.*, 2006), and blocking the deactivation of Rad53 by deletion of PPH3 promotes filamentous growth and increased virulence (Sun *et al.*, 2011; Feng *et al.*, 2013, 2017). Deletion of RTT109, which plays critical roles in maintaining genome stability, results in fungal cells that are significantly less pathogenic in mice and more susceptible to killing by macrophages *in vitro* than wild-type (WT) cells (Lopes da Rosa *et al.*, 2010). While foundational *C. albicans* DNA damage response studies have been performed, there is a need for more systematic studies of the DNA damage response given its known role in virulence.

To enhance our understanding of DNA damage repair in *C. albicans*, we screened the GRACE collection of tet-repressible conditional mutations (Roemer *et al.*, 2003) for MMS sensitivity. We

identified 56 strains that were sensitive after repression of the regulated gene. Among these strains, we were intrigued that loss of Hof1, a protein previously shown to play a critical function in cytokinesis, led to MMS sensitivity. To better understand the potential function of Hof1 in the DNA damage pathway, we used genetic approaches to characterize the function of Hof1. This work suggests there is interplay between Hof1 and the Rad53-mediated checkpoint.

## RESULTS

### Large-scale identification of MMS-sensitive strains in *C. albicans*

To identify MMS-sensitive *C. albicans* strains, the GRACE strains (Roemer *et al.*, 2003) were conditionally repressed on tetracycline-containing (100 µg/ml) YPD plates with MMS (0.01% vol/vol) and grown at 30°C for 72 h. We identified 56 strains from the 2357 single mutants of the GRACE collection that were sensitive to MMS on repression (Figure 1). Close to half of those sensitive mutants identified were components of the cell division machinery, with roles in DNA replication, DNA damage repair, and cytokinesis. Genes involved in transcription and RNA processing accounted for a further one-third of the sensitive strains while the remaining genes were involved in translation, protein processing, cellular transport, and biosynthetic pathways.

### HOF1 deletion results in sensitivity to genotoxic stress

The GRACE library screening showed conditional inactivation of Hof1-rendered cells sensitive to MMS. In *S. cerevisiae*, Hof1 is a well-studied protein implicated in regulating actin organization, cytokinesis, and secretory vesicle trafficking (Vallen *et al.*, 2000; Blondel *et al.*, 2005; Meitinger *et al.*, 2011; Wang *et al.*, 2018). In *C. albicans*, previous research reported a similar function for Hof1 in cytokinesis (Li *et al.*, 2006). Since Hof1 is predicted to be cytokinesis-related, MMS sensitivity on loss of HOF1 was unexpected. To investigate the DNA damage-related function of Hof1 in *C. albicans*, we deleted HOF1 in the SN148 background using a CRISPR/Cas9 system.

Cells lacking HOF1 had an abnormal morphology consistent with the role of Hof1 in cytokinesis. Most *hof1/hof1* cells were elongated and connected (Figure 2A). Indeed, quantification of

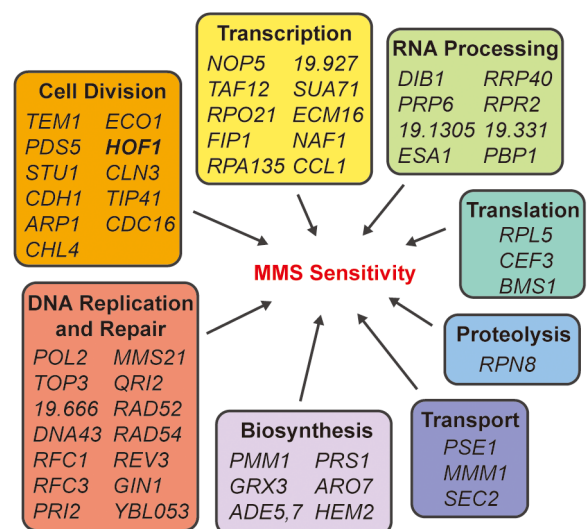


**FIGURE 1:** Identification of MMS-sensitive mutants from GRACE library screening. The 56 mutants that were scored as sensitive to MMS under tetracycline shutoff are shown, clustered by their predicted cellular processes.

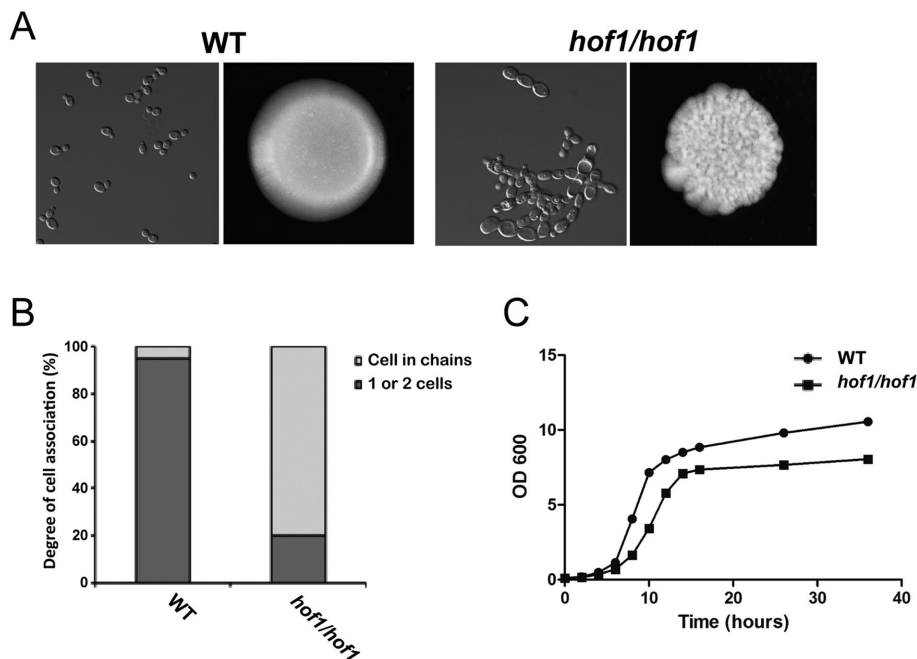


**FIGURE 2:** Strains lacking *HOF1* display cell division defects. (A) Wild-type and *hof1/hof1* strains were grown in YPD media and imaged with DIC optics (left images) or grown on YPD plates to image colony morphology (right images). (B) Percentage of cells in chains was determined by imaging cells grown in YPD.  $N \geq 200$ /condition. (C) Growth curves of wild-type and *hof1/hof1* strains were made by measuring OD<sub>600</sub> at the indicated time points. For each strain, three isolates were tested and the average is displayed.

cell chains with three or more cells revealed that 80% of *Hof1* deletion cells were in chains versus 5% in WT cells (Figure 2B). On plates, *HOF1* deletion colonies showed irregular surfaces and edges (Figure 2A). Deletion of *HOF1* also reduced the growth rate (Figure 2C).

Consistent with our screen, *hof1/hof1* cells were MMS sensitive and this phenotype could be complemented (Figure 3A). Furthermore, the *HOF1* deletion strain was sensitive to other DNA replication stresses including HU and to UV light (Figure 3A). These results suggest *Hof1* plays a general role in the response to genotoxic stress.

To test the function of *Hof1* in mediating genomic stability, we designed a heterozygous *URA3*<sup>+</sup> strain to investigate loss of heterozygosity through a 5-fluoroorotic acid (5-FOA) resistance assay. We found that the WT strain has a relatively low frequency of losing the *URA3* marker ( $3.7 \times 10^{-5}$ ), while the *HOF1* deletion strain has a roughly 20-fold higher frequency of loss ( $6.7 \times 10^{-4}$ ), indicating *Hof1* plays a role in maintaining genome stability (Figure 3B).

As *Hof1*-modulated morphological changes may be associated with the DNA damage response, we treated WT and

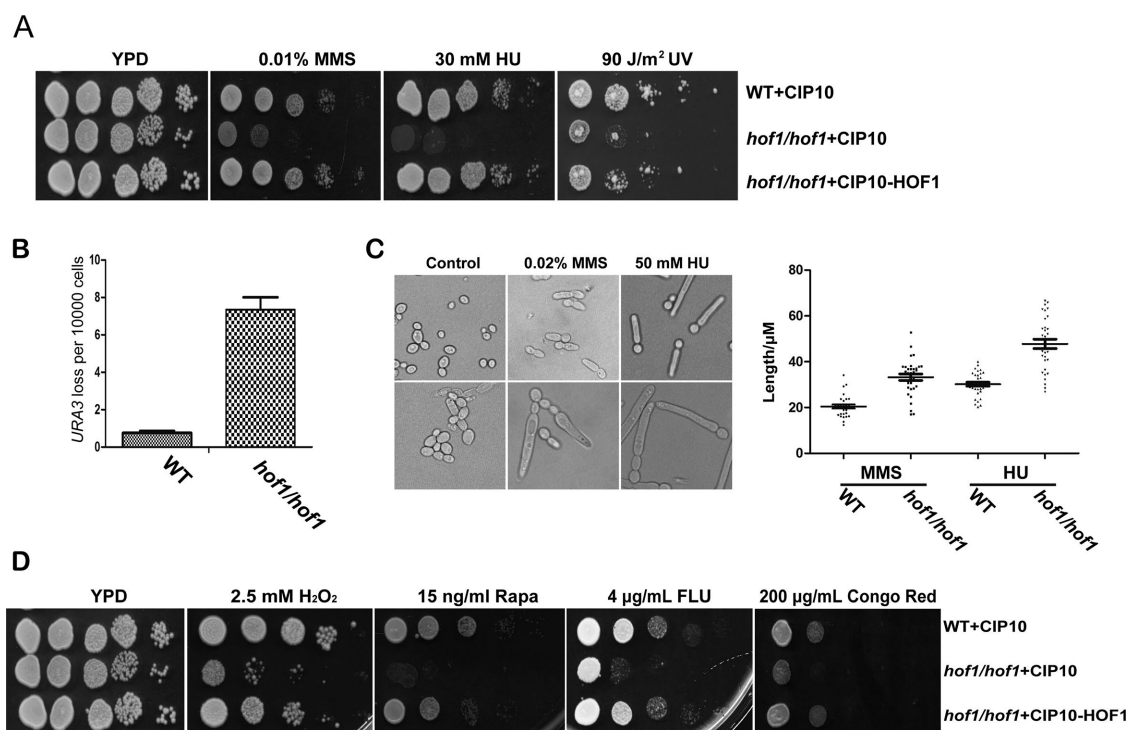
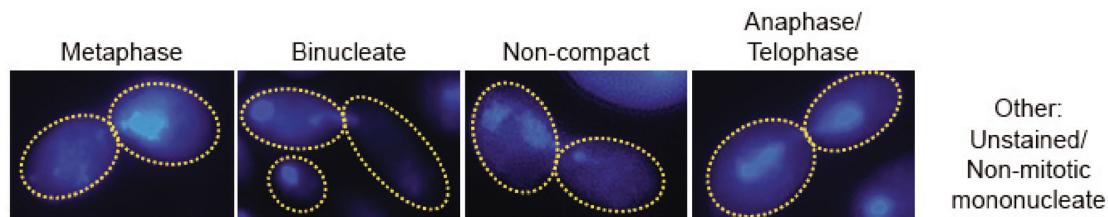


**FIGURE 3:** Deletion of *HOF1* causes sensitivity to genotoxic stress and increases genome instability. (A) *hof1/hof1* cells are sensitive to genotoxic stresses MMS, HU, and UV light. Growth assays with WT (WT+CIP10), *HOF1* deletion (*hof1/hof1*+CIP10), and *HOF1* deletion-complemented (*hof1/hof1*+CIP10-*HOF1*) strains. (B) The frequency of losing a heterozygous *URA3* marker was assessed by comparing the number of colonies on YNB+ 5-FOA and YPD plates;  $n = 3$ . (C) WT and *HOF1* deletion strains were treated with 0.02% MMS or 50 mM HU and imaged after 3 h (MMS) or 6 h (HU). Bud length was measured by ImageJ software;  $>30$  cells/condition. (D) Growth assays in the presence of H<sub>2</sub>O<sub>2</sub>, rapamycin, fluconazole, and Congo red.



	Untreated				
WT	16.5 ± 4.5	0.5 ± 0.5	1.5 ± 0.5	21.5 ± 4.5	60.0 ± 8.0
<i>rad53/rad53</i>	19.5 ± 3.5	3.0 ± 1.0	5.0 ± 5.0	20.5 ± 8.5	51.5 ± 5.5
<i>hof1/hof1</i>	8.0 ± 3.0	25.5 ± 5.5	9.0 ± 0	15.0 ± 1.0	41.5 ± 2.5
<i>rad53/rad53hof1/hof1</i>	10.0 ± 3.0	10.5 ± 2.5	5.0 ± 2.0	6.5 ± 1.5	67.5 ± 1.5
	+0.02% MMS				
WT	58.5 ± 6.5	0	2.0 ± 2.0	10.5 ± 3.5	29.0 ± 1.0
<i>rad53/rad53</i>	13.0 ± 1.0	14.0 ± 2.0	15.0 ± 1.0	17.0 ± 3.0	41.0 ± 1.0
<i>hof1/hof1</i>	18.0 ± 2.0	15.0 ± 0.0	7.0 ± 0	10.0 ± 1.0	50.0 ± 1.0
<i>rad53/rad53hof1/hof1</i>	8.5 ± 2.5	14.0 ± 1.0	13.5 ± 1.5	27.0 ± 2.0	37.0 ± 1.0

MMS-treated or untreated cells were stained with DAPI to show nuclear structure. Cells with nuclear structures that fell into one of four categories (metaphase, anaphase/telophase, binucleate, or noncompact nuclei) were identified, and the relative fraction of each category was determined;  $n = 2$ ,  $\geq 52$  cells/condition per replicate.

**TABLE 1:** Nuclear segregation in *HOF1* and/or *RAD53* deletion cells.

*HOF1* deletion cells with 0.02% MMS and 50 mM HU for 6 h before checking the cell morphology. Both WT and *hof1/hof1* cells were elongated after the treatments (Figure 3C). However, compared with the WT strain, the *HOF1* deletion cells were substantially longer, suggesting loss of Hof1 exacerbates morphological defects associated with genotoxic stress.

Given that genome instability may be associated with nuclear segregation defects, we compared nuclear segregation in WT and *HOF1* deletion cells with or without MMS treatment. To facilitate the comparison, 4',6'-diamidino-2-phenylindole dihydrochloride (DAPI)-stained cells were binned into categories of metaphase, anaphase/telophase, abnormal binucleate, noncompact nuclei, and other, which captured poorly stained and G1/S/G2 mononucleate cells. In the absence of MMS, only 2% of WT cells showed abnormal binucleate or noncompact nuclei structures while *hof1/hof1* cells were highly abnormal, with 34.5% of cells either binucleate or containing noncompact nuclei (Table 1). Notably, only 23% of the *hof1/hof1* cells were visibly undergoing mitosis, which was a substantial reduction relative to both WT (38%) and suggests slower progression through G1/S/G2. When cells were treated with MMS, WT cells largely arrested in metaphase (58.5%), whereas *hof1/hof1* cells (18%) did not arrest effectively and the binucleate/noncompact nuclei phenotypes persisted. Thus, *hof1/hof1* cells display impeded cell cycle progression, show high levels of binucleate cells consistent with defective cytokinesis, and are poorly competent for MMS-triggered metaphase arrest.

We further checked whether Hof1 plays a role in the response to other cellular stresses. We found *HOF1* deletion renders cells sensitive to 2.5 mM H<sub>2</sub>O<sub>2</sub>, 15 ng/ml rapamycin, 4 μg/ml fluconazole, and 200 mg/ml Congo red (Figure 3D). These results suggest Hof1 may be involved in responding to a variety of stresses.

### Functional analysis of Hof1 domains

In *S. cerevisiae*, the N terminus of Hof1 is implicated in control of cell size and actin cable levels, while the C terminus controls actin cable organization via regulation of the formin Bnr1 (Kamei *et al.*, 1998; Graziano *et al.*, 2014). Alignments show that the amino acid

sequence of CaHof1 has only 15% identity with ScHof1. However, the proteins have a similar domain structure (Figure 4A): an N-terminal F-BAR domain (11–266 amino acids), containing an FCH domain (13–102 amino acids), and a C-terminal SH3 domain (539–605 amino acids). To further investigate how Hof1 may function in the DNA damage response, we checked cell morphology and sensitivity to genotoxic stress in strains lacking a single Hof1 domain each.

Deletion of the F-BAR domain, but not the SH3 domain, resulted in defects of similar severity to a *hof1/hof1* mutant. Cells with a SH3 domain deletion were morphologically similar to the WT, while deletion of the F-BAR domain resulted in numerous cell chains and morphology similar to *HOF1* deletion cells (Figure 4B). Furthermore, the F-BAR deletion, but not the SH3 deletion, caused sensitivity to both MMS and HU, suggesting the F-BAR domain is required for both the response to DNA damage and the maintenance of cell morphology while the SH3 domain is dispensable (Figure 4C).

To test whether the F-BAR deletion (Hof1ΔF-BAR) may cause the above phenotypes indirectly by destabilizing Hof1, we checked the expression of Hof1 and Hof1ΔF-BAR by Western blotting (Figure 4D). Deletion of the F-BAR domain strongly reduced Hof1 levels. Furthermore, the levels of both Hof1 and Hof1ΔF-BAR decreased significantly on 0.02% MMS treatment (Figure 4D), and the levels were further reduced at higher MMS concentrations (unpublished data). Thus, the dysfunction caused by the F-BAR deletion can be partially explained by the destabilization of Hof1. Since the Hof1 levels decreased in cells treated with MMS, we also checked Hof1 levels in response to other stresses. Hof1 levels were down-regulated in response to HU, H<sub>2</sub>O<sub>2</sub>, rapamycin, and NaCl (Figure 4E). By contrast, a significant up-regulation of Hof1 protein level was observed in response to Congo red, which may reflect a targeted response by Hof1 to cell wall stress.

### Genetic interaction analysis of *HOF1* with DNA damage-related genes

In *S. cerevisiae*, MMS sensitivity of a *HOF1* deletion strain has been reported based on high throughput screening results



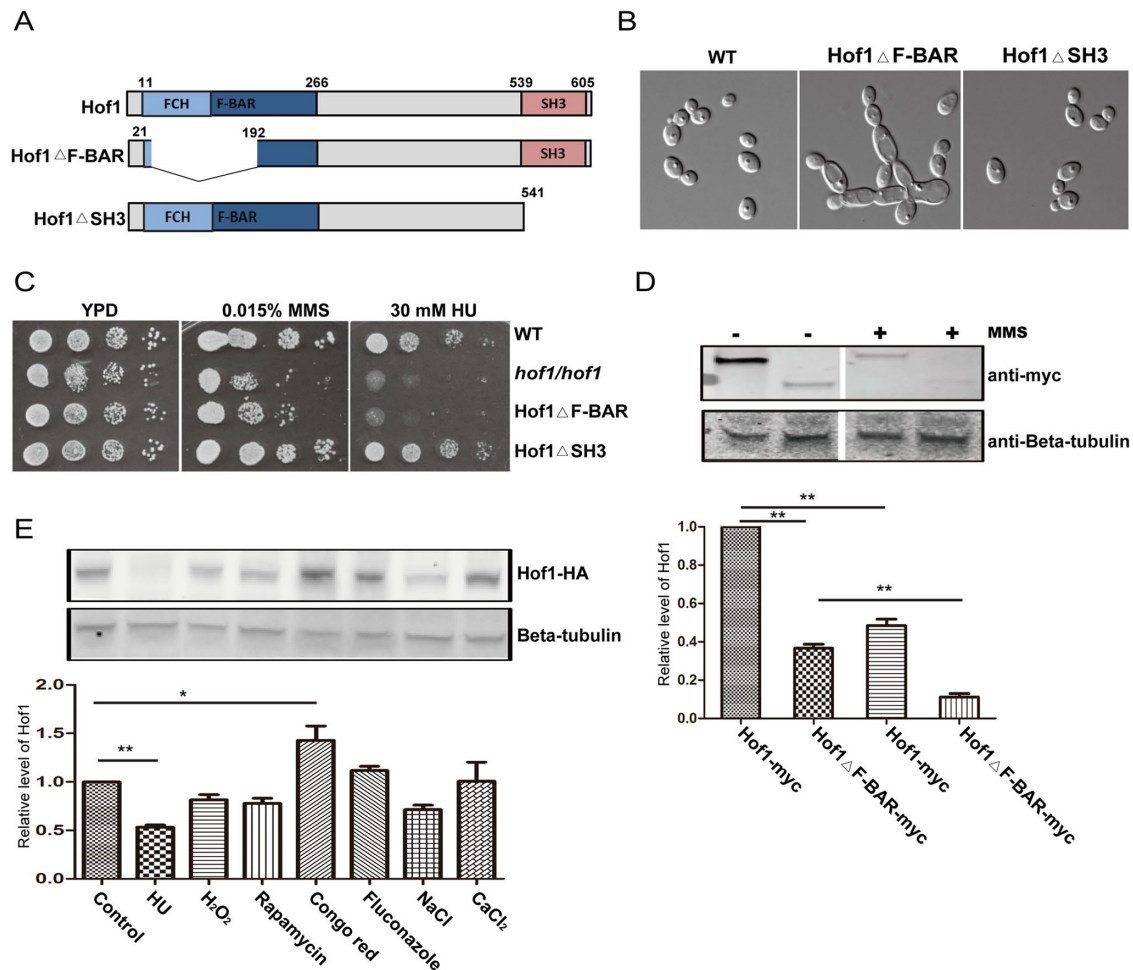


**FIGURE 4:** Functional analysis of the Hof1 F-BAR and SH3 domains. (A) Schematics of *C. albicans* Hof1 and the Hof1ΔF-BAR and Hof1ΔSH3 mutants. (B) Cell morphologies of WT and Hof1 mutant strains grown in YPD imaged with DIC optics. (C) Growth assays of WT and Hof1 mutant strains in the presence of genotoxic stresses. (D) Western blot of samples from log phase Hof1-myc and Hof1ΔF-BAR-myc cultures showing expression levels in the absence and presence of MMS (0.02% for 90 min). β-Tubulin is a loading control, and normalized band intensities are shown below. (E) Expression of Hof1-HA tested by Western blotting after treating log phase cells with 40 mM HU, 2.5 mM H<sub>2</sub>O<sub>2</sub>, 10 nM rapamycin, 100 μg/ml Congo red, 5 μg/ml fluconazole, 1.5 M NaCl, or 200 mM CaCl<sub>2</sub> for 90 min before lysis. Control cells were untreated and Hof1 was probed using an anti-HA antibody. β-Tubulin acts as a loading control and normalized band intensities are shown below. Two-tailed t test;  $n = 3$ ; \*\* $P < 0.01$ ; \* $P < 0.05$ .

(Chang *et al.*, 2002; Svensson *et al.*, 2011), but no specific function in the DNA damage response pathway was assigned to Hof1. To better understand the role of Hof1 in response to DNA damage in *C. albicans*, a genetic interaction analysis was performed.

To do so, a series of DNA damage repair gene deletions and double deletions, also lacking *HOF1*, were made. Rad53, a main checkpoint kinase in *C. albicans* (Shi *et al.*, 2007), was chosen to address a potential role of Hof1 in DNA damage signal transduction. We also deleted *PPH3*, a catalytic subunit of protein phosphate 4, which controls Rad53 deactivation during the recovery from or adaptation to DNA damage (Sun *et al.*, 2011; Feng *et al.*, 2017). Rad18, of the Rad6 epistasis group, was chosen as a component of postreplication repair (Bailey *et al.*, 1997). Mms22, a putative adaptor subunit of an E3 ubiquitin ligase complex, represented the replication repair pathway (Yan *et al.*, 2015). Mms21, a potential SUMO E3 ligase, was chosen to check the potential function of Hof1 in the SUMO-related DNA repair pathway, and Rad52 represented the homologous DNA recombination group (Lisby *et al.*, 2001). Siz1

is a potential homologue of the ScSiz1 SUMO E3 ligase, which is functionally distinct from Mms21 and helps address DNA damage in the absence of Nfi1 (Takahashi *et al.*, 2006). Rad14, Rad4, and Rad23 represented the NER group where Rad14 is part of the NER1 complex and Rad4 and Rad23 are part of NER2.

Removal of any of Rad18, Mms21, Mms22, Pph3, Rad52, or Rad14 resulted in an MMS-sensitive phenotype, and the sensitivity to MMS of double mutants of Hof1 with Rad18, Mms21, Mms22, Rad52, Pph3, or Rad14 was increased relative to the single mutants (Figure 5A), suggesting Hof1 acts independent of those proteins in the MMS response. By contrast, while the *RAD53* deletion strain was MMS sensitive, additional deletion of *HOF1* did not result in increased MMS sensitivity, suggesting Rad53 and Hof1 may act in a similar pathway (Figure 5B). The *SIZ1* deletion strain was not MMS sensitive even at high concentrations (unpublished data), nor did *SIZ1* deletion affect *hof1/hof1* sensitivity, indicating Siz1 does not play a role in responding to MMS (Figure 5C). Neither the *RAD4* nor the *RAD23* deletion strains showed sensitivity to MMS, but strikingly

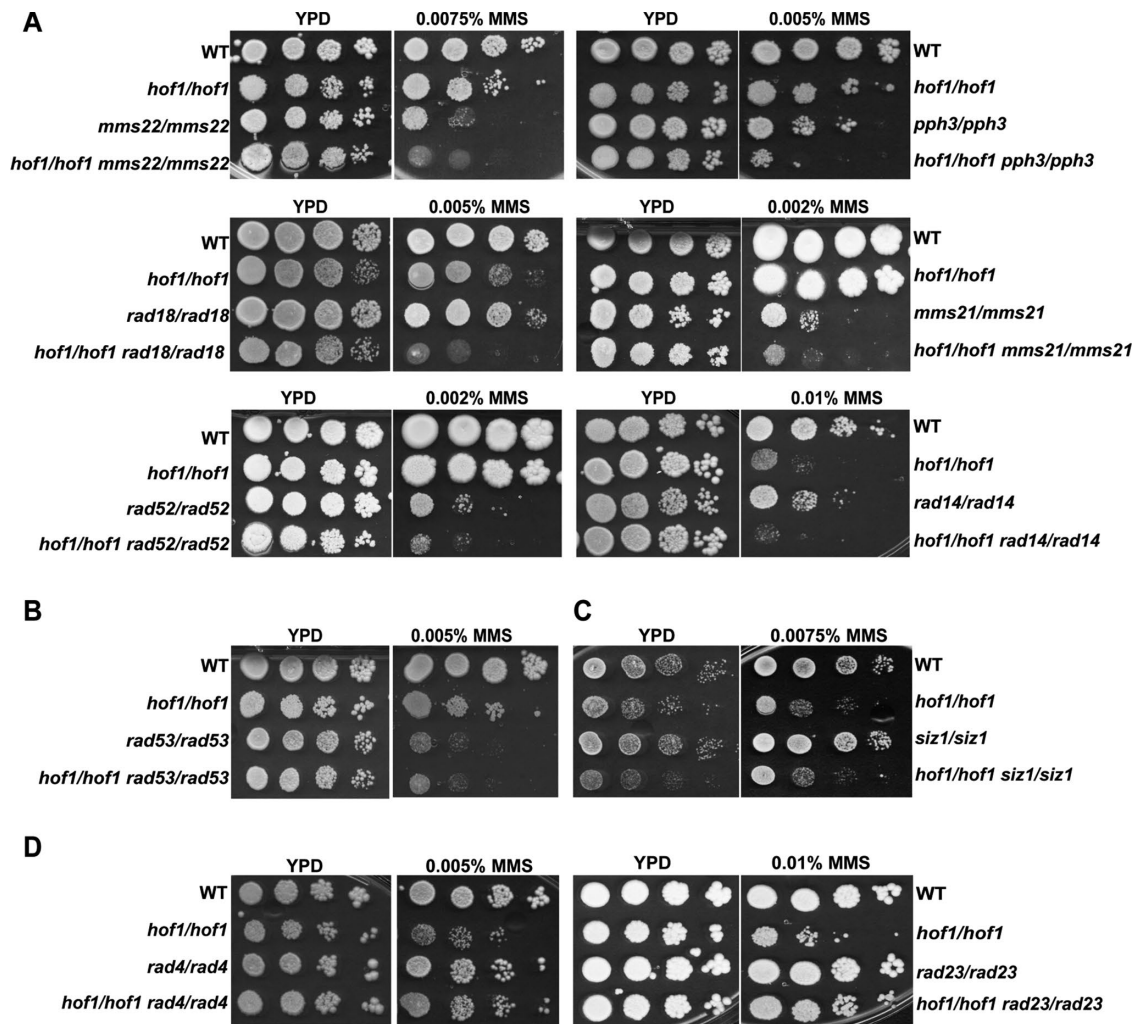


**FIGURE 5:** Genetic epistasis analysis of *HOF1*. Growth assays show MMS sensitivity increases on double deletion of *HOF1* and *MMS22*, *PPH3*, *MMS21*, *RAD18*, *RAD52*, or *RAD14* (A), but not in the double deletions of *HOF1* with *RAD53* (B) or *SIZ1* (C). (D) Deletion of *RAD23* or *RAD4* rescues *hof1/hof1* MMS sensitivity.

both deletions were able to rescue *hof1/hof1* MMS sensitivity (Figure 5D). This indicates *hof1/hof1* MMS sensitivity is suppressed by loss of *RAD4* or *RAD23*. Taken together, these results suggest that Hof1 shows a role in MMS response independent of Rad18, Mms21, Mms22, Rad52, Rad14, and Pph3, but appears to be part of the Rad53 checkpoint kinase-related circuit, and the requirement of Hof1 in this circuit for repair of MMS damage is greatly reduced on *RAD4* or *RAD23* deletion.

### Interplay between Hof1 and the Rad53 circuit

Our genetic interaction data suggest Hof1 is associated with the Rad53 circuit. In *C. albicans*, Rad53 is a main checkpoint kinase; it is activated by phosphorylation in response to DNA damage and inactivated by dephosphorylation after repair (Yao *et al.*, 2017). Blocking activation or inactivation of the checkpoint leads to DNA damage sensitivity (O'Neill *et al.*, 2007; Fiorani *et al.*, 2008). Given the Hof1–Rad53 association, we checked Rad53 behavior in a *HOF1* deletion background. Previously, we reported that Rad53 is phosphorylated in response to MMS, resulting in a slower migration rate in SDS–PAGE (Feng *et al.*, 2013). Here, we found that Rad53 was phosphorylated after MMS exposure in both WT and *HOF1* deletion strains (Figure 6A). After removal of MMS, Rad53

could be dephosphorylated in both backgrounds. Taken together, *HOF1* deletion has no dramatic impact on the activation or deactivation of Rad53.

We next asked whether Rad53 modulates the behavior of Hof1. As the level of the Hof1 protein is down-regulated in response to MMS (Figure 4D), we tested whether this could be influenced by Rad53. While *RAD53* deletion has no impact on the level of Hof1 in untreated cells, *RAD53* deletion stabilizes Hof1 levels after MMS treatment (Figure 6B). Thus, *RAD53* deletion blocked the MMS-induced reduction of Hof1 levels. *RAD53* deletion also exhibited a similar stabilizing effect on Hof1 levels in the presence of HU (Supplemental Figure S1). Rad53 may directly stabilize Hof1 in the presence of these genotoxic stresses, or increased Hof1 levels may be a result of disabling the Rad53-mediated DNA repair checkpoint, releasing cells from a phase where Hof1 levels are normally depressed. To differentiate between these possibilities, WT cells expressing Hof1-HA and GFP-tagged tubulin (Tub2-GFP) were synchronized by MMS exposure, released, and both Hof1-HA levels and spindle length were tracked (Supplemental Figure S2). After MMS exposure, Hof1-HA levels are depressed, but they recover within 3 h as the cell cycle progresses, denoted by increasing spindle length. Taking the results together, Hof1 levels are

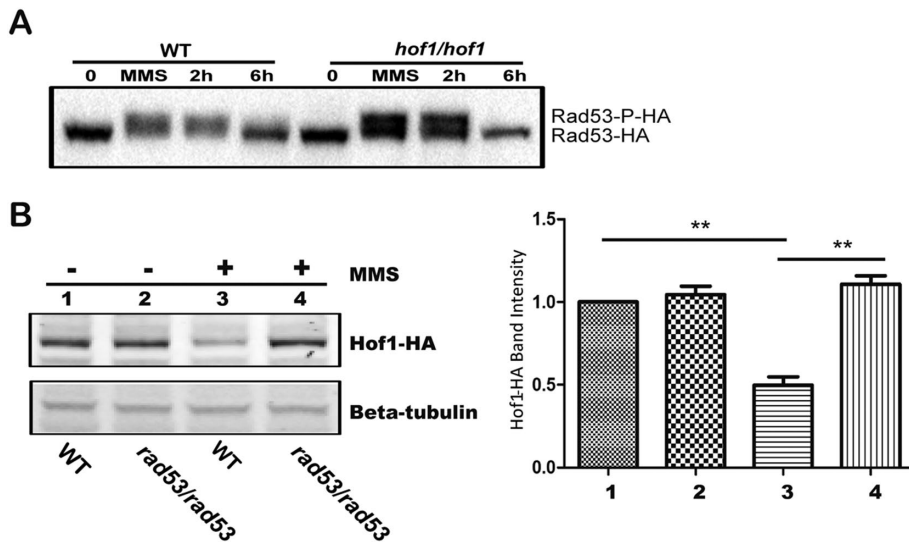


**FIGURE 6:** Checkpoint kinase Rad53 modulates Hof1 levels. (A) Anti-HA Western blot of WT and *hof1/hof1* strains with Rad53-HA that were incubated with 0.02% MMS for 90 min (MMS), resuspended in YPD, and further incubated for indicated times (2 and 6 h). Untreated cells (0) were included as controls. (B) Western blot of Hof1-HA in WT and a *RAD53* deletion strain with and without a 90-min 0.02% MMS treatment. Hof1-HA was probed using an anti-HA antibody, and  $\beta$ -tubulin was a loading control. Band intensities relative to WT untreated are shown. Two-tailed t test;  $n = 3$ ;  $**P < 0.01$ .

modified by Rad53, though the effect may be an indirect effect of halting the cell cycle at a phase with lowered Hof1 levels.

We further investigated the influence of Rad53 and Hof1 on checkpoint-mediated, MMS-induced cell cycle arrest by microscopy. As previously noted, DAPI-stained cells were binned into categories of metaphase, anaphase/telophase, abnormal binucleate, noncompact nuclei, and other, which captured poorly stained and G1/S/G2 mononucleate cells. As shown in Table 1, treatment of WT cells with 0.02% MMS caused efficient arrest (58.5% metaphase). In contrast, while the *RAD53* deletion has almost no effect on the distribution of untreated cells, MMS-treated cells do not arrest efficiently (only 13% metaphase), similar to previous findings (Shi *et al.*, 2007), and there is a substantial population of abnormal cells (29% binucleate and noncompact nuclei). Likewise, the *HOF1* deletion strain did not show a substantial arrest on MMS exposure (18% metaphase). When a *RAD53 HOF1* double deletion was imaged there was no indication of cell cycle arrest after MMS treatment (8.5% metaphase), though there were somewhat fewer abnormal cells when untreated (8% vs. 34.5% for *hof1/hof1* mutants), suggesting *RAD53* deletion had a moderating influence on the *hof1/hof1* strain. Notably, many more *RAD53 HOF1* double deletion cells were observed in anaphase/telophase than in either single deletion (27% vs. 17% or 10%) on MMS treatment, suggesting possible defects in late stage mitosis. Overall, *HOF1* and *RAD53* deletions have remarkably similar effects on MMS-induced metaphase arrest, consistent with their association in the DNA damage response.

### Rad23 rescues MMS sensitivity of *HOF1* deletions

Through the genetic interaction assays (Figure 5), we noted *RAD23* deletion rescued *hof1/hof1* MMS sensitivity. To confirm this phenotype, we performed a quantitative survival assay by counting viable cells after 2 h MMS treatment (Figure 7A). As previously observed, deletion of *HOF1* decreased MMS survival, deletion of *RAD23* increased MMS survival, and the *HOF1 RAD23* double deletion strain

had MMS resistance similar to the *RAD23* deletion strain. This further demonstrates that loss of Rad23 rescues MMS sensitivity caused by loss of Hof1.

To establish whether this rescue is specific for MMS, we also checked the phenotype of the above mutants under other genotoxic stresses. Loss of *RAD23* rescued *hof1/hof1* HU sensitivity, suggesting *RAD23* deletion may suppress the sensitivity of *hof1/hof1* cells to a range of stresses. In contrast, the *HOF1* and *RAD23* double deletion strain showed nearly the same sensitivity as the *RAD23* deletion strain to UV light indicating there is some specificity in the Rad23-mediated rescue of *HOF1* deletion phenotypes (Figure 7B). Similar results were obtained for a *HOF1* and *RAD4* double deletion strain (unpublished data). Since Hof1 is a cytokinesis-related protein, we asked whether loss of Rad23 could rescue the observed defects of *HOF1* strains in cell division. We found that the *HOF1 RAD23* double deletion strain showed similar cellular and colony morphology to that of the *HOF1* deletion strain (Figure 7C). Thus, the ability of *RAD23* deletion to suppress *hof1*

mutant phenotypes is limited to repressing DNA damage sensitivity and does not extend to the cytokinesis defect.

In *S. cerevisiae*, Rad23 is critical for NER, is part of a ubiquitin/proteasome pathway, and has been shown to repress DNA damage response genes (Reed and Gillette, 2007; Zhou *et al.*, 2015). Owing to its regulatory role of DNA damage response genes and since decreased proteasome function enables increased DNA repair (Lommel *et al.*, 2000), we tested whether *RAD23* deletion increases Rad53 levels (Figure 7D). Indeed, we found elevated Rad53 levels in a *RAD23* deletion and a *RAD23 HOF1* double deletion strain, but not in a *HOF1* deletion strain. Thus, the *RAD23* deletion-mediated rescue of a *HOF1* deletion strain could be caused by increased repair efficiency resulting from elevated Rad53 levels. To test whether high Rad53 levels can rescue *hof1* mutant MMS sensitivity, we substituted the *RAD53* promoter with the strong *MET3* promoter and measured MMS sensitivity. As shown in Figure 7E, *RAD53* overexpression partially rescued *hof1* mutant sensitivity to MMS and HU.

### DISCUSSION

Our screen of the GRACE library for MMS sensitivity has uncovered many elements of the *C. albicans* DNA damage response network. By pursuing one unexpected hit, cytokinesis regulator Hof1, we have characterized a link between cytokinesis and DNA damage response. *HOF1* deletion causes MMS sensitivity and genome instability, and Hof1 is not only genetically associated with the Rad53 pathway but also its levels drop in a Rad53-dependent manner in response to MMS. The role of Hof1 appears to be coordinated with other aspects of the DNA damage response, given that the importance of Hof1 in the MMS response is reduced in Rad23 or Rad4 mutant strains and when Rad53 is overexpressed.

Overall, our screen identified several genes, including *HOF1*, that do not appear to be directly connected to DNA repair. Establishing the connection of these genes to sensitivity to MMS treatment should expand our understanding of the complex



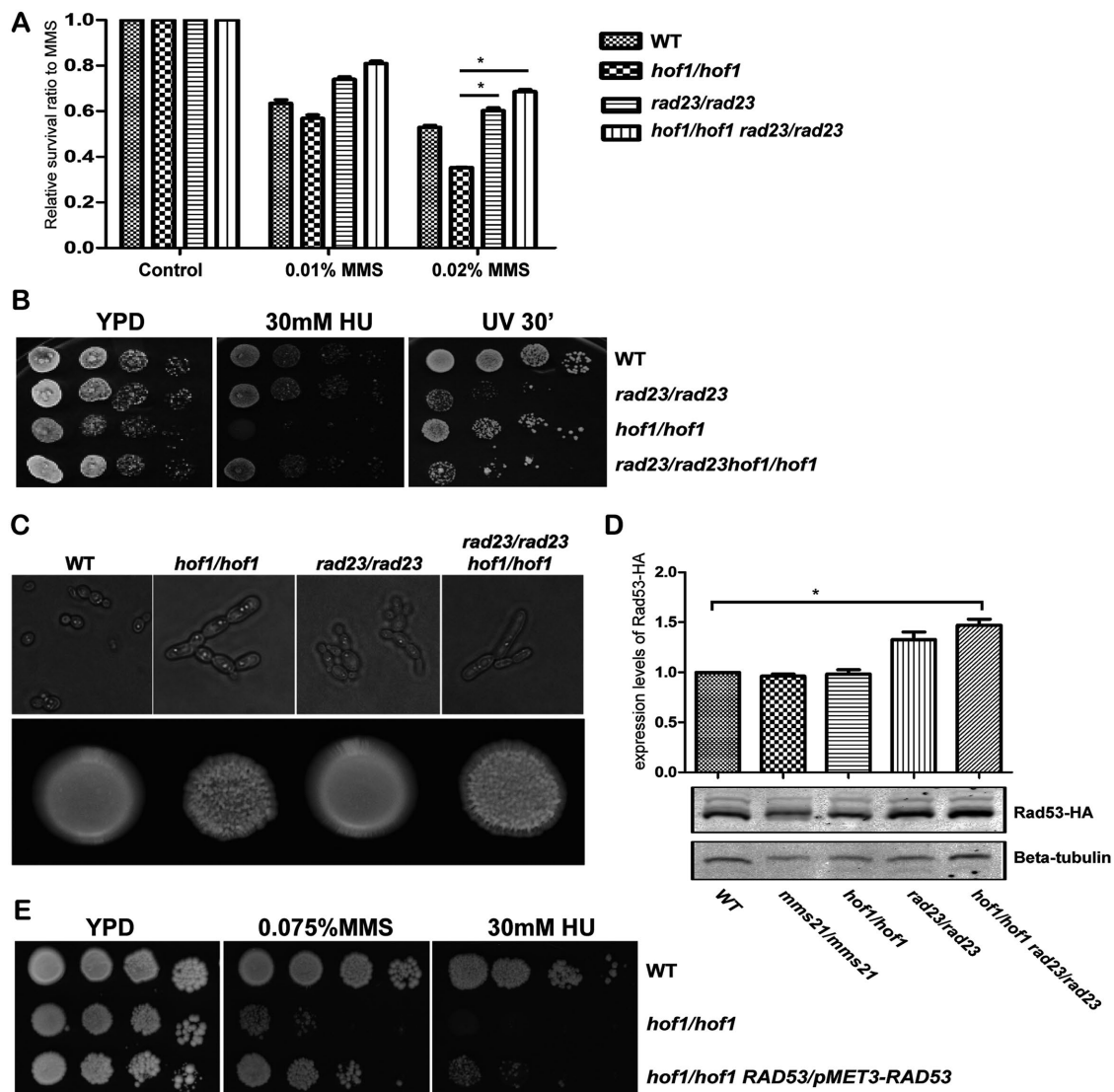


**FIGURE 7: RAD23 deletion rescues *hof1/hof1* MMS sensitivity.** (A) The indicated strains were treated with either 0.01% MMS or 0.02% MMS for 2 h prior to dilution and dispersion on YPD plates to measure survival. Colonies were counted and compared with untreated control cells. (B) Growth assays measuring *hof1/hof1* and *rad23/rad23* sensitivity to HU and UV. (C) Images of the indicated strains in YPD media (top) or on YPD plates (bottom). (D) RAD23 deletion can elevate Rad53 levels. Anti-HA Western blot of the indicated deletion strains with Rad53-HA.  $\beta$ -Tubulin is a loading control. Rad53 band intensities were measured and normalized to WT cells. Two-tailed t test;  $n = 3$ ;  $*P < 0.05$ . (E) Growth assay showing that elevated expression of Rad53 suppresses *hof1/hof1* sensitivity to MMS and HU.

relationships between cellular repair and functions linked to processes such as metabolism and cell cycle control.

In *S. cerevisiae*, the physical interactions of Hof1 with septins and actin during septum formation and the role of Hof1 in cytokinesis have been well characterized (Vallen *et al.*, 2000; Blondel *et al.*, 2005). In *C. albicans*, Hof1 is also reported to function in cytokinesis (Li *et al.*, 2006). We confirmed *HOF1* deletion causes cell division defects and explored a novel role for Hof1 in MMS tolerance. Since cytokinesis occurs late in the cell cycle, typically after DNA replication, the function of Hof1 in response to DNA damage may be distinct from its role from cytokinesis. We found Hof1 protein levels decrease in response to the stressors MMS, HU,  $H_2O_2$ , and rapamycin. RNA sequence analysis indicates MMS lowers *HOF1* expression ( $\log_2$  fold change =  $-1.48$ ,  $P < 0.001$ ; unpublished data), suggesting Hof1 levels are transcriptionally regulated to some extent. In contrast, Hof1 levels increased in response to the

cell wall-damaging agent Congo red. This contrasting impact on Hof1 levels may be due to a link between cytokinesis and wall remodeling. Furthermore, the ability of *rad4* and *rad23* mutants to suppress *hof1* mutant MMS sensitivity, but not cell division defects, supports the possibility of distinct roles for Hof1 in damage repair and in cytokinesis.

While Hof1 may have two distinct functions, the cell wall integrity and DNA repair pathways may also modulate Hof1 indirectly. For example, DNA damage could halt the cell cycle earlier, resulting in lowering Hof1 expression, whereas damage to the cell wall may necessitate an increase in Hof1 levels, or greater time preparing for cell division, to ensure cell wall integrity. In this model, loss of Hof1 may decrease control of the cell cycle, increasing the likelihood of irreparable damage in the presence of either type of stressor. In any case, there is a logic to linking the DNA damage checkpoint to regulation of cytokinesis, and though the roles of Hof1 in damage



regulation and cytokinesis might not overlap completely, they may be connected.

The MMS-induced decrease in Hof1 levels does appear to be checkpoint related given its dependence on the main DNA damage checkpoint kinase Rad53. In the initial response to MMS, Rad53 is activated while Hof1 levels are suppressed. However, the reduction of Hof1 levels is not as persistent; after a 3 h MMS treatment followed by a 2-h wash out, Rad53 remains in its active phosphorylated form, while Hof1 protein levels have recovered (unpublished data). This suggests Hof1 depression is more transient during DNA damage. Importantly, we also found that Hof1 levels fluctuate during the cell cycle and appear to be depressed in S phase when the Rad53-mediated repair checkpoint occurs (Supplemental Figure S1). This suggests indirect regulation of Hof1 by Rad53, whose deletion may lead to abnormal cell cycle regulation as the cell compensates for its loss. While there is evidence that the Hof1–Rad53 interaction is indirect, the fact that our cell synchronization assay depended on MMS for synchronization is a confounding factor as it may have also driven more direct down-regulation of Hof1. To better tease apart this relationship, new approaches to cell synchronization in *C. albicans* are required. Even if Rad53 regulation of Hof1 is primarily indirect, we cannot exclude the role of Hof1 in the checkpoint-related DNA damage response.

We found that deletion of the NER components, Rad4 and Rad23, partially rescued *hof1* mutant MMS sensitivity. In *S. cerevisiae*, Rad4 and Rad23 can bind the promoters of a subset of DNA damage-responsive genes, repressing their expression (Zhou *et al.*, 2015). The slightly increased Rad53 protein levels observed in both *rad23* and *hof1 rad23* mutants could be explained by the derepression of *RAD53* transcription caused by loss of Rad23. Thus, one explanation for suppression of MMS sensitivity by *RAD4* or *RAD23* deletions is that their loss increases Rad53 levels, elevating the rate of DNA repair and cell survival under MMS stress. Alternatively, Rad4 and Rad23 have been shown to heavily down-regulate Dun1, a G2/M checkpoint kinase downstream of Rad53 required for DNA damage-induced cell cycle arrest and previously shown to down-regulate Hof1 in *S. cerevisiae* (Zhou *et al.*, 2015). The elevated levels of Dun1 resulting from loss of Rad4/23 may itself be enough to stall the cell cycle, allowing DNA repair independent of a direct action of Rad4/23 on Rad53. In either case, loss of Rad4/23 accelerates DNA repair or stalls the cell cycle, which likely proceeds independent of Hof1, allowing suppression of MMS sensitivity.

We propose a speculative model to explain the connection of Hof1 to MMS damage repair (Figure 8). In this model Rad53 is activated in response to DNA damage and lowers Hof1 levels indirectly or directly, blocking cell cycle progression to ensure time to repair damaged DNA. Here Hof1 may act as a core component of the cytokinesis machinery to link DNA damage repair to cytokinesis through its responsiveness to the checkpoint kinase Rad53 either directly, or indirectly, through Rad53 effectors such as Dun1 (Jaehnig *et al.*, 2013). Previously, both Enserink *et al.* (2006) and Smolka *et al.* (2006) have demonstrated a potential close association between Rad53 and the septin machinery required for cytokinesis in *S. cerevisiae*. Hof1 may play a role in this linkage or act in a parallel pathway to restrict cytokinesis in the presence of DNA damage. In either case, deletion of *HOF1* induces MMS sensitivity through poor regulation of cytokinesis, potentially exacerbated by weakening the Rad53-mediated checkpoint. Poorly controlled cytokinesis may either take longer, allowing the accumulation of further mutations, or proceed rapidly, before mutations can be repaired. The need for Hof1 can

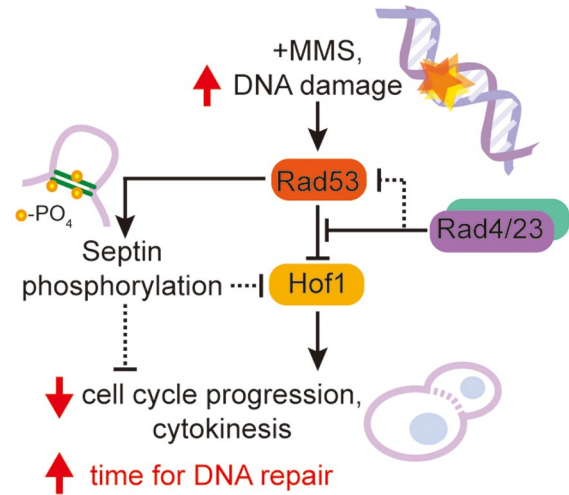


**FIGURE 8:** Hypothetical model of the Hof1, Rad53, and Rad4/Rad23 regulatory network in *C. albicans*. A potential regulatory network that explains how a DNA damage signal propagates through Rad53 and subsequently Hof1 to regulate the cell cycle. Note that Rad53 may also act through septin phosphorylation according to work in *S. cerevisiae* and Rad4/23 may act to depress signal transduction either downstream of Rad53 or of Rad53 itself. Solid lines indicate interactions (direct or indirect) previously identified in *S. cerevisiae* while dotted arrows are hypothetical. Arrows represent activation, while bars represent inhibition.

be bypassed by accelerating DNA repair by overexpressing Rad53 or deleting Rad4/23.

Potentially, Hof1 could act as a necessary additional signal for Rad53 activation, though its presence at the cell periphery and its cell cycle-dependent expression make it an unlikely candidate to detect DNA damage. Here, deletion of Hof1 or inactivation of Rad53 leads to similar levels of damage sensitivity, and the *rad53 hof1* double mutant has an equivalent sensitivity to either single mutant. This would position Hof1 as a timer for the checkpoint, eventually shutting off the Rad53-induced checkpoint and resetting the normal cell cycle.

In this study, we establish that the cytokinesis regulator Hof1 is genetically linked to the Rad53 checkpoint kinase in *C. albicans*. Loss of Hof1 leads to enhanced DNA damage sensitivity, yet the Rad53 response to MMS in part acts by decreasing Hof1 levels, likely through an indirect pathway. Hof1 thus appears to be a potential component linking the DNA damage checkpoint and cytokinesis. Further work is needed to fully unravel the details of Hof1 molecular regulation and the link to the Rad53 checkpoint.

## MATERIALS AND METHODS

### Strains, media, and reagents

The *C. albicans* strains were grown in yeast extract peptone dextrose (YPD) medium with 50 mg uridine/l as described (MacPherson *et al.*, 2005). Strains and primers used in this study are listed in Supplemental Tables S1 and S2. MMS was purchased from Sigma (USA). HU and other chemicals were purchased from Bioshop (Canada). The yeast nitrogen base (YNB) medium was supplemented with appropriate nutrients for plasmids selection and maintenance. Solid media contained 2% agar.

### GRACE library MMS sensitivity assay

The GRACE library was transferred from frozen glycerol stocks into 96-well plates containing liquid YPD with 200  $\mu$ g/ml nourseothricin

using sterile 96 pin replicators and incubated overnight at 30°C. Overnight cultures were spotted, using a 96 pin replicator, onto YPD agar, YPD agar with tetracycline (100 µg/ml), and YPD agar with tetracycline-added MMS (0.01% vol/vol). Plates were incubated at 30°C for 3 d, and strains that were growing well on tetracycline but not on plates with both tetracycline and MMS were scored as sensitive. Sensitivity of those strains was further confirmed by making 10-fold dilutions of overnight cultures in sterile distilled water and then plating 5 µl of each dilution on tetracycline and tetracycline plus MMS plates. Images of plates and colonies were scanned at 300 dots per inch using an Epson Perfection v500 photo scanner.

### Gene deletion, rescue, and epitope tagging of proteins

To construct a *HOF1* deletion strain in *C. albicans*, we used a CRISPR/Cas9 system (Vyas *et al.*, 2015). The small guide RNA (sgRNA) of *HOF1* was formed by annealing primers HOF1-sg-F and HOF1-sg-R and cloning the resulting ds fragment into the *BsmBI* site of pV1093 to generate plasmid pV1093-Hof1-sgRNA. A repair DNA fragment, containing the *HIS1* marker, was amplified with primers HOF1-Re-F and HOF1-Re-R using pFA-HIS1 as a template. The pV1093-Hof1-sgRNA was then linearized with *SacI* and *KpnI* and transformed into *C. albicans* strain SN148 together with the *HOF1* repair DNA. Transformants were selected on YNB-his plus 200 µg/ml nourseothricin. The knockout strains were confirmed with primers HOF1-Te-F and HOF1-Te-R. To rescue the phenotype of *HOF1* deletion strain, a 3031-base pair DNA fragment containing the full-length *HOF1* gene was amplified with primers HOF1-Te-F and HOF1-Te-R and cloned into the *KpnI* site of plasmid CIP10 (Murad *et al.*, 2000), generating pCIP10-HOF1. Then, pCIP10-HOF1 was linearized by *StuI* and integrated into the RP10 locus of the genome. The integration was confirmed using primers URA-TF and RPS-F.

Similarly, a transient CRISPR/Cas9 system (Min *et al.*, 2016) was used to knock out *MMS22*, *RAD18*, *RAD52*, *RAD53*, *RAD14*, *RAD4*, *RAD23*, and *SIZ1* in SN148 or the *HOF1* deletion strain. Generally, a Cas9 gene was amplified with common primers P7 and P8. The sgRNA was amplified by annealing PCR with primers P5 and P6, using the products of two separate PCR reactions containing the sgRNA sequence, and repair DNA was amplified from pFA-ARG4. Finally, the Cas9, sgRNA and repair DNA products were transformed into either the WT or the Hof1 deletion strain and selected on SD-Arg plates. The correct knockout strains were confirmed by PCR.

To construct the *PPH3 HOF1* double deletion strain, a previous *PPH3* deletion strain (Feng *et al.*, 2013) was used as a background strain and a similar CRISPR/Cas9 system for *HOF1* was used. Similarly, a *MMS21* deletion strain constructed before (Islam *et al.*, 2019) was used as a background strain to construct the *MMS21 HOF1* double deletion strain.

To construct the *RAD53* overexpression strain, a MET3 promoter was amplified from pFA-URA3-MET3 to substitute the original promoter of *RAD53* gene.

To test the expression of the Hof1 protein, a MYC or HA tag was amplified from the pFA-MYC-URA or pFA-HA-URA plasmids and integrated at the 3' end of the *HOF1* gene using the CRISPR/Cas9 system, generating a homozygous *HOF1*-MYC or *HOF1*-HA strain. Similarly, a HA tag was integrated into the 3' end of the *RAD53* gene using the CRISPR/Cas9 system. The integration was confirmed by both PCR and by Western blotting.

To check the spindle morphology, a GFP tag was amplified from the pFA-GFP-URA plasmid and integrated at the 3' end of the *TUB2* gene in SN148 background.

### Protein extraction, Western blot, and immunoprecipitation (IP)

Exponentially growing cells were harvested by centrifugation and ~100 mg of cells were suspended in 200 µl of ice-cold RIPA buffer (50 mM Tris, pH 7.4, 150 mM NaCl, 1% NP-40, EDTA-free protease inhibitor mix [Roche], and phosphatase inhibitor cocktail [Roche]) (Gao *et al.*, 2014). After an equal volume of acid-washed glass beads was added, cells were broken by five rounds of 60 s of beating, with 5 min of cooling on ice between rounds, using a FastPrep-24 Disruptor. The supernatant was collected after centrifugation of the cell lysate at 12,000 rpm for 10 min at 4°C. Protein concentrations were determined using a BCA protein assay (Feng *et al.*, 2013). Western blot analysis was carried out as described (Feng *et al.*, 2017).

For the IP assays, anti-MYC beads (QED Bioscience) (10 µl) were washed twice with RIPA buffer and incubated with 5 mg total protein extract in 1 ml extraction buffer at 4°C overnight. Next morning, beads were harvested and washed three times with 1 ml RIPA buffer. Proteins were subjected to Western blot analysis as above using rabbit monoclonal anti-MYC antibody (QED Bioscience) to detect Hof1-MYC.

To detect Rad53-HA, a rabbit monoclonal anti-HA antibody (QED Bioscience) and the goat anti-rabbit immunoglobulin G secondary antibody were purchased from ODSEY and processed as described above for the anti-MYC antibody.

### Growth assay

Cells were grown overnight in liquid YPD medium at 30°C, serially diluted by 10-fold, and spotted onto solid plates containing stress chemicals. Plates were incubated for 2–3 d at 30°C before scanning by an Epson Perfection v500 photo scanner.

### Genome stability assay

To assess genome stability (Kumaran *et al.*, 2013), the CIP10 plasmid (Murad *et al.*, 2000) containing a *URA* marker was linearized by *StuI* and integrated into the RP10 locus of both WT and *HOF1* deletion strains, generating heterozygous *URA3* strains. The strains were streaked on YNB dextrose-ura twice and inoculated in YPD overnight at 30°C. Next day, cells were harvested and washed twice with distilled water; 10-fold dilutions were made before spotting. For each strain, 10<sup>-1</sup> cells (100 µl) were spotted on YNB dextrose 5-FOA plates while 10<sup>-4</sup> cells (20 µl) were spotted on YPD plates to check the cell numbers. All the strains were grown as duplicates in three independent samples. Finally, the average numbers of cells on YNB dextrose 5-FOA plates and YPD plates were calculated.

### Microscopy

Overnight cells were diluted down to an OD<sub>600</sub> of 0.2 in YPD with and without 0.02% MMS and incubated for 6 h. To visualize DNA, cells were fixed in fresh 70% ethanol for 20 min, washed with sterile water, incubated in 1.0 µg/ml DAPI (Sigma-Aldrich) for 20 min, washed twice with sterile water, and mounted on slides. Cells were imaged on a Leica DM6000B microscope (Leica Microsystems Canada, Richmond Hill, ON, Canada) equipped with a Hamamatsu-ORCA ER camera (Hamamatsu Photonics, Hamamatsu City, Japan) and the HCX PL APO 63× NA 1.40-0 oil or the HCX PLFLUO TAR 100× NA 1.30-0.6 oil objectives. Differential interference contrast (DIC) optics or epifluorescence with DAPI (460 nm) filters were utilized. Images were captured with Volocity software (Improvision, Perkin-Elmer, Waltham, MA).

### ACKNOWLEDGMENTS

We thank all the members of Whiteway lab for the helpful discussion, and we thank Merck for access to the Grace collection of

regulated gene disruptions. This work was supported by the Natural Science Foundation of Nantong City to J.F. (No. JC2018052), Natural Sciences and Engineering Research Council of Canada (NSERC) grants to M.W. (CRC 950-228957 and discovery RGPIN/4799), the Priority Academic Program Development of Jiangsu Higher Education Institutions, and a Jiangsu government scholarship for overseas studies, China.

## REFERENCES

- Andaluz E, Ciudad T, Gomez-Raja J, Calderone R, Larriba G (2006). Rad52 depletion in *Candida albicans* triggers both the DNA-damage checkpoint and filamentation accompanied by but independent of expression of hypha-specific genes. *Mol Microbiol* 59, 1452–1472.
- Bacal J, Moriel-Carretero M, Pardo B, Barthe A, Sharma S, Chabes A, Lengronne A, Pasero P (2018). Mrc1 and Rad9 cooperate to regulate initiation and elongation of DNA replication in response to DNA damage. *EMBO J* 37, e99319.
- Bailly V, Lauder S, Prakash S, Prakash L (1997). Yeast DNA repair proteins Rad6 and Rad18 form a heterodimer that has ubiquitin conjugating, DNA binding, and ATP hydrolytic activities. *J Biol Chem* 272, 23360–23365.
- Baroni E, Viscardi V, Cartagena-Lirola H, Lucchini G, Longhese MP (2004). The functions of budding yeast Sae2 in the DNA damage response require Mec1- and Tel1-dependent phosphorylation. *Mol Cell Biol* 24, 4151–4165.
- Berens TJ, Toczyski DP (2012). Colocalization of Mec1 and Mrc1 is sufficient for Rad53 phosphorylation in vivo. *Mol Biol Cell* 23, 1058–1067.
- Blondel M, Bach S, Bamps S, Dobbelaere J, Wiget P, Longaretti C, Barral Y, Meijer L, Peter M (2005). Degradation of Hof1 by SCF(Grr1) is important for actomyosin contraction during cytokinesis in yeast. *EMBO J* 24, 1440–1452.
- Boiteux S, Jinks-Robertson S (2013). DNA repair mechanisms and the bypass of DNA damage in *Saccharomyces cerevisiae*. *Genetics* 193, 1025–1064.
- Branzei D, Foiani M (2006). The Rad53 signal transduction pathway: Replication fork stabilization, DNA repair, and adaptation. *Exp Cell Res* 312, 2654–2659.
- Chang M, Bellaoui M, Boone C, Brown GW (2002). A genome-wide screen for methyl methanesulfonate-sensitive mutants reveals genes required for S phase progression in the presence of DNA damage. *Proc Natl Acad Sci USA* 99, 16934–16939.
- Chen H, Donnianni RA, Handa N, Deng SK, Oh J, Timashev LA, Kowalczykowski SC, Symington LS (2015). Sae2 promotes DNA damage resistance by removing the Mre11-Rad50-Xrs2 complex from DNA and attenuating Rad53 signaling. *Proc Natl Acad Sci USA* 112, E1880–E1887.
- Conde F, Ontoso D, Acosta I, Gallego-Sanchez A, Bueno A, San-Segundo PA (2010). Regulation of tolerance to DNA alkylating damage by Dot1 and Rad53 in *Saccharomyces cerevisiae*. *DNA Repair (Amst)* 9, 1038–1049.
- Enserink JM, Smolka MB, Zhou H, Kolodner RD (2006). Checkpoint proteins control morphogenetic events during DNA replication stress in *Saccharomyces cerevisiae*. *J Cell Biol* 175, 729–741.
- Feng J, Duan Y, Qin Y, Sun W, Zhuang Z, Zhu D, Jiang L (2017). The N-terminal pY33XL motif of CaPsy2 is critical for the function of protein phosphatase 4 in CaRad53 deactivation, DNA damage-induced filamentation and virulence in *Candida albicans*. *Int J Med Microbiol* 307, 471–480.
- Feng J, Zhao Y, Duan Y, Jiang L (2013). Genetic interactions between protein phosphatases CaPtc2p and CaPph3p in response to genotoxins and rapamycin in *Candida albicans*. *FEMS Yeast Res* 13, 85–96.
- Fiorani S, Mimun G, Caleca L, Piccini D, Pellicoli A (2008). Characterization of the activation domain of the Rad53 checkpoint kinase. *Cell Cycle* 7, 493–499.
- Gao XJ, Feng JX, Zhu S, Liu XH, Tardieux I, Liu LX (2014). Protein phosphatase 2C of *Toxoplasma gondii* interacts with human SSRP1 and negatively regulates cell apoptosis. *Biomed Environ Sci* 27, 883–893.
- Graziano BR, Yu HY, Alioto SL, Eskin JA, Ydenberg CA, Waterman DP, Garabedian M, Goode BL (2014). The F-BAR protein Hof1 tunes formin activity to sculpt actin cables during polarized growth. *Mol Biol Cell* 25, 1730–1743.
- Hanway D, Chin JK, Xia G, Oshiro G, Winzeler EA, Romesberg FE (2002). Previously uncharacterized genes in the UV- and MMS-induced DNA damage response in yeast. *Proc Natl Acad Sci USA* 99, 10605–10610.
- Heideker J, Lis ET, Romesberg FE (2007). Phosphatases, DNA damage checkpoints and checkpoint deactivation. *Cell Cycle* 6, 3058–3064.
- Hoeijmakers JH (2009). DNA damage, aging, and cancer. *N Engl J Med* 361, 1475–1485.
- Islam A, Tebbji F, Mallick J, Regan H, Dumeaux V, Omran RP, Whiteway M (2019). Mms21: a putative SUMO E3 ligase in *Candida albicans* that negatively regulates invasiveness and filamentation, and is required for the genotoxic and cellular stress response. *Genetics* 211, 579–595.
- Jaehnig EJ, Kuo D, Hombauer H, Ideker TG, Kolodner RD (2013). Checkpoint kinases regulate a global network of transcription factors in response to DNA damage. *Cell Rep* 4, 174–188.
- Kamei T, Tanaka K, Hihara T, Umikawa M, Imamura H, Kikyo M, Ozaki K, Takai Y (1998). Interaction of Bnr1p with a novel Src homology 3 domain-containing Hof1p. Implication in cytokinesis in *Saccharomyces cerevisiae*. *J Biol Chem* 273, 28341–28345.
- Kim JA, Hicks WM, Li J, Tay SY, Haber JE (2011). Protein phosphatases pph3, ptc2, and ptc3 play redundant roles in DNA double-strand break repair by homologous recombination. *Mol Cell Biol* 31, 507–516.
- Kitanovic A, Wolf S (2006). Fructose-1,6-bisphosphatase mediates cellular responses to DNA damage and aging in *Saccharomyces cerevisiae*. *Mutat Res* 594, 135–147.
- Kumaran R, Yang SY, Leu JY (2013). Characterization of chromosome stability in diploid, polyploid and hybrid yeast cells. *PLoS One* 8, e68094.
- Kwon Y, Sung P (2017). Rad52, maestro of inverse strand exchange. *Mol Cell* 67, 1–3.
- Lawrence C (1994). The RAD6 DNA repair pathway in *Saccharomyces cerevisiae*: what does it do, and how does it do it? *Bioessays* 16, 253–258.
- Leroy C, Lee SE, Vaze MB, Ochsenbein F, Guerois R, Haber JE, Marsolier-Kergoat MC (2003). PP2C phosphatases Ptc2 and Ptc3 are required for DNA checkpoint inactivation after a double-strand break. *Mol Cell* 11, 827–835.
- Li WJ, Wang YM, Zheng XD, Shi QM, Zhang TT, Bai C, Li D, Sang JL, Wang Y (2006). The F-box protein Grr1 regulates the stability of Ccn1, Cln3 and Hof1 and cell morphogenesis in *Candida albicans*. *Mol Microbiol* 62, 212–226.
- Lisby M, Rothstein R, Mortensen UH (2001). Rad52 forms DNA repair and recombination centers during S phase. *Proc Natl Acad Sci USA* 98, 8276–8282.
- Loll-Kripplleber R, d'Enfert C, Feri A, Diogo D, Perin A, Marcet-Houben M, Bounoux ME, Legrand M (2014). A study of the DNA damage checkpoint in *Candida albicans*: uncoupling of the functions of Rad53 in DNA repair, cell cycle regulation and genotoxic stress-induced polarized growth. *Mol Microbiol* 91, 452–471.
- Lommel L, Chen L, Madura K, Sweder K (2000). The 26S proteasome negatively regulates the level of overall genomic nucleotide excision repair. *Nucleic Acids Res* 28, 4839–4845.
- Lopes da Rosa J, Boyartchuk VL, Zhu LJ, Kaufman PD (2010). Histone acetyltransferase Rtt109 is required for *Candida albicans* pathogenesis. *Proc Natl Acad Sci USA* 107, 1594–1599.
- Lundin C, North M, Erixon K, Walters K, Jenssen D, Goldman AS, Helleday T (2005). Methyl methanesulfonate (MMS) produces heat-labile DNA damage but no detectable in vivo DNA double-strand breaks. *Nucleic Acids Res* 33, 3799–3811.
- MacPherson S, Akache B, Weber S, De Deken X, Raymond M, Turcotte B (2005). *Candida albicans* zinc cluster protein Upc2p confers resistance to antifungal drugs and is an activator of ergosterol biosynthetic genes. *Antimicrob Agents Chemother* 49, 1745–1752.
- Meitinger F, Boehm ME, Hofmann A, Hub B, Zentgraf H, Lehmann WD, Pereira G (2011). Phosphorylation-dependent regulation of the F-BAR protein Hof1 during cytokinesis. *Genes Dev* 25, 875–888.
- Memisoglu A, Samson L (2000). Base excision repair in yeast and mammals. *Mutat Res* 451, 39–51.
- Min K, Ichikawa Y, Woolford CA, Mitchell AP (2016). *Candida albicans* gene deletion with a transient CRISPR-Cas9 system. *mSphere* 1, e00130-16.
- Murad AM, Lee PR, Broadbent ID, Barelle CJ, Brown AJ (2000). Clp10, an efficient and convenient integrating vector for *Candida albicans*. *Yeast* 16, 325–327.
- Murakami-Sekimata A, Huang D, Piening BD, Bangur C, Paulovich AG (2010). The *Saccharomyces cerevisiae* RAD9, RAD17 and RAD24 genes are required for suppression of mutagenic post-replicative repair during chronic DNA damage. *DNA Repair (Amst)* 9, 824–834.
- Ohouo PY, Bastos de Oliveira FM, Liu Y, Ma CJ, Smolka MB (2013). DNA-repair scaffolds dampen checkpoint signalling by counteracting the adaptor Rad9. *Nature* 493, 120–124.

- O'Neill BM, Szyjka SJ, Lis ET, Bailey AO, Yates JR 3rd, Aparicio OM, Romesberg FE (2007). Pph3-Psy2 is a phosphatase complex required for Rad53 dephosphorylation and replication fork restart during recovery from DNA damage. *Proc Natl Acad Sci USA* 104, 9290–9295.
- Pelliccioli A, Foiani M (2005). Signal transduction: how rad53 kinase is activated. *Curr Biol* 15, R769–R771.
- Prakash S, Prakash L (2000). Nucleotide excision repair in yeast. *Mutat Res* 451, 13–24.
- Reed SH, Gillette TG (2007). Nucleotide excision repair and the ubiquitin proteasome pathway—do all roads lead to Rome? *DNA Repair (Amst)* 6, 149–156.
- Roemer T, Jiang B, Davison J, Ketela T, Veillette K, Breton A, Tandia F, Linteau A, Sillaots S, Marta C, et al. (2003). Large-scale essential gene identification in *Candida albicans* and applications to antifungal drug discovery. *Mol Microbiol* 50, 167–181.
- Sanchez Y, Desany BA, Jones WJ, Liu Q, Wang B, Elledge SJ (1996). Regulation of RAD53 by the ATM-like kinases MEC1 and TEL1 in yeast cell cycle checkpoint pathways. *Science* 271, 357–360.
- Schwartz MF, Duong JK, Sun Z, Morrow JS, Pradhan D, Stern DF (2002). Rad9 phosphorylation sites couple Rad53 to the *Saccharomyces cerevisiae* DNA damage checkpoint. *Mol Cell* 9, 1055–1065.
- Shi QM, Wang YM, Zheng XD, Lee RT, Wang Y (2007). Critical role of DNA checkpoints in mediating genotoxic-stress-induced filamentous growth in *Candida albicans*. *Mol Biol Cell* 18, 815–826.
- Sirbu BM, Cortez D (2013). DNA damage response: three levels of DNA repair regulation. *Cold Spring Harb Perspect Biol* 5, a012724.
- Smolka MB, Chen SH, Maddox PS, Enserink JM, Albuquerque CP, Wei XX, Desai A, Kolodner RD, Zhou H (2006). An FHA domain-mediated protein interaction network of Rad53 reveals its role in polarized cell growth. *J Cell Biol* 175, 743–753.
- Somasagara RR, Spencer SM, Tripathi K, Clark DW, Mani C, Madeira da Silva L, Scalici J, Kothayer H, Westwell AD, Rocconi RP, et al. (2017). RAD6 promotes DNA repair and stem cell signaling in ovarian cancer and is a promising therapeutic target to prevent and treat acquired chemoresistance. *Oncogene* 36, 6680–6690.
- Sun LL, Li WJ, Wang HT, Chen J, Deng P, Wang Y, Sang JL (2011). Protein phosphatase Pph3 and its regulatory subunit Psy2 regulate Rad53 dephosphorylation and cell morphogenesis during recovery from DNA damage in *Candida albicans*. *Eukaryot Cell* 10, 1565–1573.
- Svensson JP, Pesudo LQ, Fry RC, Adeleye YA, Carmichael P, Samson LD (2011). Genomic phenotyping of the essential and non-essential yeast genome detects novel pathways for alkylation resistance. *BMC Syst Biol* 5, 157.
- Sweeney FD, Yang F, Chi A, Shabanowitz J, Hunt DF, Durocher D (2005). *Saccharomyces cerevisiae* Rad9 acts as a Mec1 adaptor to allow Rad53 activation. *Curr Biol* 15, 1364–1375.
- Takahashi Y, Yong-Gonzalez V, Kikuchi Y, Strunnikov A (2006). SIZ1/SIZ2 control of chromosome transmission fidelity is mediated by the sumoylation of topoisomerase II. *Genetics* 172, 783–794.
- Vallen EA, Caviston J, Bi E (2000). Roles of Hof1p, Bni1p, Bnr1p, and myo1p in cytokinesis in *Saccharomyces cerevisiae*. *Mol Biol Cell* 11, 593–611.
- Vyas VK, Barrasa MI, Fink GR (2015). A *Candida albicans* CRISPR system permits genetic engineering of essential genes and gene families. *Sci Adv* 1, e1500248.
- Wang M, Nishihama R, Onishi M, Pringle JR (2018). Role of the Hof1-Cyk3 interaction in cleavage-furrow ingression and primary-septum formation during yeast cytokinesis. *Mol Biol Cell* 29, 597–609.
- Weinert TA, Kiser GL, Hartwell LH (1994). Mitotic checkpoint genes in budding yeast and the dependence of mitosis on DNA replication and repair. *Genes Dev* 8, 652–665.
- Whiteway M, Bachewich C (2007). Morphogenesis in *Candida albicans*. *Annu Rev Microbiol* 61, 529–553.
- Wood RD, Mitchell M, Sgouros J, Lindahl T (2001). Human DNA repair genes. *Science* 291, 1284–1289.
- Yan L, Xiong J, Lu H, Lv QZ, Ma QY, Cote P, Whiteway M, Jiang YY (2015). The Role of Mms22p in DNA damage response in *Candida albicans*. *G3 (Bethesda)* 5, 2567–2578.
- Yao G, Wan J, Liu Q, Mu C, Wang Y, Sang J (2017). Characterization of Pph3-mediated dephosphorylation of Rad53 during methyl methane-sulfonate-induced DNA damage repair in *Candida albicans*. *Biochem J* 474, 1293–1306.
- Zhou BB, Elledge SJ (2000). The DNA damage response: putting checkpoints in perspective. *Nature* 408, 433–439.
- Zhou Z, Humphries N, van Eijk P, Waters R, Yu S, Kraehenbuehl R, Hartsuiker E, Reed SH (2015). UV induced ubiquitination of the yeast Rad4-Rad23 complex promotes survival by regulating cellular dNTP pools. *Nucleic Acids Res* 43, 7360–7370.